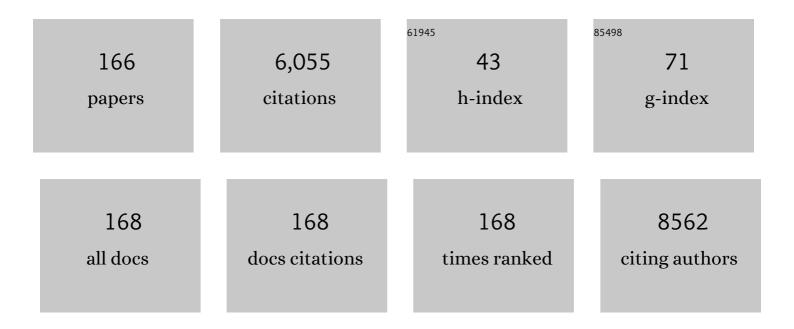
List of Publications by Year in descending order

Source: https://exaly.com/author-pdf/8148475/publications.pdf Version: 2024-02-01



D K CIDI

#	Article	IF	CITATIONS
1	Evidence of oxygen vacancy induced room temperature ferromagnetism in solvothermally synthesized undoped TiO2 nanoribbons. Nanoscale, 2013, 5, 5476.	2.8	258
2	Correlation between microstructure and optical properties of ZnO nanoparticles synthesized by ball milling. Journal of Applied Physics, 2007, 102, .	1.1	228
3	Interfacial charge transfer in oxygen deficient TiO2-graphene quantum dot hybrid and its influence on the enhanced visible light photocatalysis. Applied Catalysis B: Environmental, 2018, 224, 960-972.	10.8	198
4	Diameter dependence of interwall separation and strain in multiwalled carbon nanotubes probed by X-ray diffraction and Raman scattering studies. Diamond and Related Materials, 2010, 19, 1281-1288.	1.8	168
5	High temperature ferromagnetism and optical properties of Co doped ZnO nanoparticles. Journal of Applied Physics, 2010, 108, .	1.1	158
6	Formation mechanism of graphene quantum dots and their edge state conversion probed by photoluminescence and Raman spectroscopy. Journal of Materials Chemistry C, 2016, 4, 10852-10865.	2.7	157
7	Signature of strong ferromagnetism and optical properties of Co doped TiO2 nanoparticles. Journal of Applied Physics, 2011, 110, .	1.1	152
8	Hydrogen Evolution Reaction Activity of Graphene–MoS ₂ van der Waals Heterostructures. ACS Energy Letters, 2017, 2, 1355-1361.	8.8	141
9	Solar light driven photoelectrocatalytic hydrogen evolution and dye degradation by metal-free few-layer MoS2 nanoflower/TiO2(B) nanobelts heterostructure. Solar Energy Materials and Solar Cells, 2018, 185, 364-374.	3.0	138
10	Structural, optical, and magnetic properties of Ni doped ZnO nanoparticles: Correlation of magnetic moment with defect density. Applied Surface Science, 2015, 356, 804-811.	3.1	133
11	Enhanced UV photosensitivity from rapid thermal annealed vertically aligned ZnO nanowires. Nanoscale Research Letters, 2011, 6, 504.	3.1	128
12	Evidence for Ti Interstitial Induced Extended Visible Absorption and Near Infrared Photoluminescence from Undoped TiO ₂ Nanoribbons: An In Situ Photoluminescence Study. Journal of Physical Chemistry C, 2013, 117, 23402-23411.	1.5	122
13	Strain induced phase formation, microstructural evolution and bandgap narrowing in strained TiO2 nanocrystals grown by ball milling. Journal of Alloys and Compounds, 2016, 676, 591-600.	2.8	121
14	Oxygen vacancy-mediated enhanced ferromagnetism in undoped and Fe-doped TiO ₂ nanoribbons. Journal Physics D: Applied Physics, 2014, 47, 235304.	1.3	115
15	Microscopic origin of lattice contraction and expansion in undoped rutile TiO ₂ nanostructures. Journal Physics D: Applied Physics, 2014, 47, 215302.	1.3	110
16	Tuning the visible photoluminescence in Al doped ZnO thin film and its application in label-free glucose detection. Sensors and Actuators B: Chemical, 2018, 254, 681-689.	4.0	96
17	Role of Surface Plasmons and Hot Electrons on the Multi-Step Photocatalytic Decay by Defect Enriched Ag@TiO ₂ Nanorods under Visible Light. Journal of Physical Chemistry C, 2017, 121, 20016-20030.	1.5	85
18	Stable p-type conductivity and enhanced photoconductivity from nitrogen-doped annealed ZnO thin film. Thin Solid Films, 2012, 520, 5000-5006.	0.8	82

#	Article	IF	CITATIONS
19	Origin of high photoluminescence yield and high SERS sensitivity of nitrogen-doped graphene quantum dots. Carbon, 2020, 160, 273-286.	5.4	82
20	Mechanism of strong visible light photocatalysis by Ag ₂ O-nanoparticle-decorated monoclinic TiO ₂ (B) porous nanorods. Nanotechnology, 2016, 27, 315703.	1.3	79
21	Room temperature ferromagnetism with high magnetic moment and optical properties of Co doped ZnO nanorods synthesized by a solvothermal route. Journal of Alloys and Compounds, 2014, 615, 378-385.	2.8	73
22	Defect Mediated Magnetic Interaction and High <l>T</l> _c Ferromagnetism in Co Doped ZnO Nanoparticles. Journal of Nanoscience and Nanotechnology, 2011, 11, 9167-9174.	0.9	69
23	Graphene-Assisted Controlled Growth of Highly Aligned ZnO Nanorods and Nanoribbons: Growth Mechanism and Photoluminescence Properties. ACS Applied Materials & Interfaces, 2014, 6, 377-387.	4.0	68
24	Role of molecular interactions and structural defects in the efficient fluorescence quenching by carbon nanotubes. Carbon, 2012, 50, 4495-4505.	5.4	67
25	Diameter dependence of oxidative stability in multiwalled carbon nanotubes: Role of defects and effect of vacuum annealing. Journal of Applied Physics, 2010, 108, .	1.1	66
26	Evolution of Nitrogen-Related Defects in Graphitic Carbon Nitride Nanosheets Probed by Positron Annihilation and Photoluminescence Spectroscopy. Journal of Physical Chemistry C, 2018, 122, 9209-9219.	1.5	66
27	Strong visible and near infrared photoluminescence from ZnO nanorods/nanowires grown on single layer graphene studied using sub-band gap excitation. Journal of Applied Physics, 2017, 122, .	1.1	63
28	Photoluminescence signature of silicon interstitial cluster evolution from compact to extended structures in ion-implanted silicon. Semiconductor Science and Technology, 2005, 20, 638-644.	1.0	62
29	On the origin of enhanced photoconduction and photoluminescence from Au and Ti nanoparticles decorated aligned ZnO nanowire heterostructures. Journal of Applied Physics, 2011, 110, 124317.	1.1	60
30	lsotype heterostructure of bulk and nanosheets of graphitic carbon nitride for efficient visible light photodegradation of methylene blue. RSC Advances, 2016, 6, 24976-24984.	1.7	60
31	Effect of ZnO seed layer on the catalytic growth of vertically aligned ZnO nanorod arrays. Materials Chemistry and Physics, 2010, 122, 18-22.	2.0	58
32	Plasmonic hole-transport-layer enabled self-powered hybrid perovskite photodetector using a modified perovskite deposition method in ambient air. Organic Electronics, 2019, 71, 175-184.	1.4	58
33	Origin of visible and near-infrared photoluminescence from chemically etched Si nanowires decorated with arbitrarily shaped Si nanocrystals. Nanotechnology, 2014, 25, 045703.	1.3	54
34	<i>In situ</i> decoration of plasmonic Au nanoparticles on graphene quantum dots-graphitic carbon nitride hybrid and evaluation of its visible light photocatalytic performance. Nanotechnology, 2017, 28, 395703.	1.3	53
35	Silicon nanowire heterostructures for advanced energy and environmental applications: a review. Nanotechnology, 2017, 28, 012001.	1.3	51
36	Solid-state synthesis of stable and color tunable cesium lead halide perovskite nanocrystals and the mechanism of high-performance photodetection in a monolayer MoS ₂ /CsPbBr ₃ vertical heterojunction. Journal of Materials Chemistry C, 2020, 8, 8917-8934.	2.7	51

#	Article	IF	CITATIONS
37	Defect Enhanced Efficient Physical Functionalization of Graphene with Gold Nanoparticles Probed by Resonance Raman Spectroscopy. Journal of Physical Chemistry C, 2014, 118, 13833-13843.	1.5	50
38	Solvent dependent synthesis of edge-controlled graphene quantum dots with high photoluminescence quantum yield and their application in confocal imaging of cancer cells. Journal of Colloid and Interface Science, 2019, 541, 387-398.	5.0	50
39	Catalyst free growth of ZnO nanowires on graphene and graphene oxide and its enhanced photoluminescence and photoresponse. Nanotechnology, 2015, 26, 145601.	1.3	49
40	Strongly enhanced visible light photoelectrocatalytic hydrogen evolution reaction in an n-doped MoS ₂ /TiO ₂ (B) heterojunction by selective decoration of platinum nanoparticles at the MoS ₂ edge sites. Journal of Materials Chemistry A, 2018, 6, 22681-22696.	5.2	49
41	Evidence for small interstitial clusters as the origin of photoluminescence W band in ion-implanted silicon. Applied Physics Letters, 2001, 78, 291-293.	1.5	48
42	Quantitative Understanding of Charge-Transfer-Mediated Fe ³⁺ Sensing and Fast Photoresponse by N-Doped Graphene Quantum Dots Decorated on Plasmonic Au Nanoparticles. ACS Applied Materials & Interfaces, 2020, 12, 4755-4768.	4.0	47
43	Precise Tuning of the Thickness and Optical Properties of Highly Stable 2D Organometal Halide Perovskite Nanosheets through a Solvothermal Process and Their Applications as a White LED and a Fast Photodetector. ACS Applied Materials & Interfaces, 2020, 12, 6283-6297.	4.0	46
44	Coupled Charge Transfer Dynamics and Photoluminescence Quenching in Monolayer MoS2 Decorated with WS2 Quantum Dots. Scientific Reports, 2019, 9, 19414.	1.6	45
45	Large exciton binding energy, high photoluminescence quantum yield and improved photostability of organo-metal halide hybrid perovskite quantum dots grown on a mesoporous titanium dioxide template. Journal of Colloid and Interface Science, 2019, 539, 619-633.	5.0	43
46	Mechanism of swelling in low-energy ion-irradiated silicon. Physical Review B, 2001, 65, .	1.1	42
47	Anomalous fluorescence enhancement and fluorescence quenching of graphene quantum dots by single walled carbon nanotubes. Physical Chemistry Chemical Physics, 2018, 20, 4527-4537.	1.3	41
48	ZnO Nanowire Heterostructures: Intriguing Photophysics and Emerging Applications. Reviews in Nanoscience and Nanotechnology, 2013, 2, 147-170.	0.4	40
49	Enhancing the Photostability of Poly(3-hexylthiophene) by Preparing Composites with Multiwalled Carbon Nanotubes. Journal of Physical Chemistry B, 2011, 115, 919-924.	1.2	39
50	Impact of reaction temperature, stirring and cosolvent on the solvothermal synthesis of anatase TiO2 and TiO2/titanate hybrid nanostructures: Elucidating theÂgrowth mechanism. Materials Chemistry and Physics, 2013, 137, 928-936.	2.0	38
51	Mesoporous Si Nanowire Templated Controlled Fabrication of Organometal Halide Perovskite Nanoparticles with High Photoluminescence Quantum Yield for Light-Emitting Applications. ACS Applied Nano Materials, 2018, 1, 1551-1562.	2.4	38
52	Direct Chemical Vapor Deposition Growth of Monolayer MoS ₂ on TiO ₂ Nanorods and Evidence for Doping-Induced Strong Photoluminescence Enhancement. Journal of Physical Chemistry C, 2018, 122, 15017-15025.	1.5	38
53	Evidence for plasmonic hot electron injection induced superior visible light photocatalysis by g-C3N4 nanosheets decorated with Ag–TiO2(B) and Au–TiO2(B) nanorods. Solar Energy Materials and Solar Cells, 2019, 201, 110053.	3.0	38
54	On the origin and tunability of blue and green photoluminescence from chemically derived graphene: Hydrogenation and oxygenation studies. Carbon, 2015, 95, 228-238.	5.4	37

#	Article	IF	CITATIONS
55	Crystalline to amorphous transition and band structure evolution in ion-damaged silicon studied by spectroscopic ellipsometry. Journal of Applied Physics, 2001, 90, 659-669.	1.1	36
56	Stacking sequence dependent photo-electrocatalytic performance of CVD grown MoS ₂ /graphene van der Waals solids. Nanotechnology, 2017, 28, 085101.	1.3	36
57	Trion-Inhibited Strong Excitonic Emission and Broadband Giant Photoresponsivity from Chemical Vapor-Deposited Monolayer MoS ₂ Grown in Situ on TiO ₂ Nanostructure. ACS Applied Materials & Interfaces, 2018, 10, 42812-42825.	4.0	36
58	Electrical characterization of MeV heavy-ion-induced damage in silicon: Evidence for defect migration and clustering. Journal of Applied Physics, 1998, 84, 1901-1912.	1.1	35
59	Multifunctional Ag nanoparticle decorated Si nanowires for sensing, photocatalysis and light emission applications. Journal of Colloid and Interface Science, 2018, 532, 464-473.	5.0	35
60	Evolution of room temperature ferromagnetism with increasing 1D growth in Ni-doped ZnO nanostructures. Journal of Alloys and Compounds, 2015, 647, 558-565.	2.8	34
61	Highly sensitive and selective label-free detection of dopamine in human serum based on nitrogen-doped graphene quantum dots decorated on Au nanoparticles: Mechanistic insights through microscopic and spectroscopic studies. Applied Surface Science, 2019, 490, 318-330.	3.1	34
62	Origin and tunability of dual color emission in highly stable Mn doped CsPbCl3 nanocrystals grown by a solid-state process. Journal of Colloid and Interface Science, 2020, 564, 357-370.	5.0	34
63	Evidence for fast decay dynamics of the photoluminescence from Ge nanocrystals embedded in SiO2. Solid State Communications, 2005, 133, 229-234.	0.9	33
64	Size-dependent visible absorption and fast photoluminescence decay dynamics from freestanding strained silicon nanocrystals. Nanoscale Research Letters, 2011, 6, 320.	3.1	33
65	Improved fast photoresponse from Al doped ZnO nanowires network decorated with Au nanoparticles. Chemical Physics Letters, 2012, 541, 39-43.	1.2	32
66	Effect of Ag/Au bilayer assisted etching on the strongly enhanced photoluminescence and visible light photocatalysis by Si nanowire arrays. Physical Chemistry Chemical Physics, 2016, 18, 7715-7727.	1.3	32
67	Mechanism of defect induced ferromagnetism in undoped and Cr doped TiO 2 nanorods/nanoribbons. Journal of Alloys and Compounds, 2016, 661, 331-344.	2.8	32
68	Strong Cathodoluminescence and Fast Photoresponse from Embedded CH3NH3PbBr3 Nanoparticles Exhibiting High Ambient Stability. ACS Applied Materials & Interfaces, 2019, 11, 14917-14931.	4.0	31
69	Recent advances in perovskite/2D materials based hybrid photodetectors. JPhys Materials, 2021, 4, 032008.	1.8	31
70	ZnO/anthracene based inorganic/organic nanowire heterostructure: Photoresponse and photoluminescence studies. Journal of Applied Physics, 2012, 111, .	1.1	29
71	Understanding the interfacial charge transfer in the CVD grown Bi ₂ O ₂ Se/CsPbBr ₃ nanocrystal heterostructure and its exploitation in superior photodetection: experiment <i>vs.</i> theory. Nanoscale, 2021, 13, 14945-14959.	2.8	28
72	RAPID THERMAL ANNEALING INDUCED ENHANCED BAND-EDGE EMISSION FROM ZnO NANOWIRES, NANORODS AND NANORIBBONS. Functional Materials Letters, 2011, 04, 25-29.	0.7	25

#	Article	IF	CITATIONS
73	Freestanding Core-Shell Nanocrystals with Varying Sizes and Shell Thicknesses: Microstructure and Photoluminescence Studies. Journal of Nanomaterials, 2012, 2012, 1-5.	1.5	25
74	Quantitative analysis of the phonon confinement effect in arbitrarily shaped Si nanocrystals decorated on Si nanowires and its correlation with the photoluminescence spectrum. Journal of Raman Spectroscopy, 2015, 46, 624-631.	1.2	25
75	Adsorption of Small Molecules on Niobium Doped Graphene: A Study Based on Density Functional Theory. IEEE Electron Device Letters, 2018, 39, 296-299.	2.2	25
76	Understanding the excitation wavelength dependent spectral shift and large exciton binding energy of tungsten disulfide quantum dots and its interaction with single-walled carbon nanotubes. Journal of Colloid and Interface Science, 2020, 561, 519-532.	5.0	25
77	Plasmon-enhanced strong visible light photocatalysis by defect engineered CVD graphene and graphene oxide physically functionalized with Au nanoparticles. Catalysis Science and Technology, 2016, 6, 7101-7112.	2.1	24
78	Aluminum doped core-shell ZnO/ZnS nanowires: Doping and shell layer induced modification on structural and photoluminescence properties. Journal of Applied Physics, 2013, 114, 134307.	1.1	23
79	Surface roughening and scaling behavior of vacuum-deposited SnCl2Pc organic thin films on different substrates. Applied Physics Letters, 2015, 107, .	1.5	23
80	Photoluminescence signature of resonant energy transfer in ZnO coated Si nanocrystals decorated on vertical Si nanowires array. Journal of Alloys and Compounds, 2015, 638, 419-428.	2.8	23
81	Ultraviolet and blue photoluminescence from sputter deposited Ge nanocrystals embedded in SiO2 matrix. Journal of Applied Physics, 2008, 103, .	1.1	22
82	Evidence for Defect-Enhanced Photoluminescence Quenching of Fluorescein by Carbon Nanotubes. Journal of Physical Chemistry C, 2011, 115, 24067-24072.	1.5	22
83	Quick single-step mechanosynthesis of ZnO nanorods and their optical characterization: milling time dependence. Applied Nanoscience (Switzerland), 2011, 1, 165-171.	1.6	22
84	Shape Tailored TiO ₂ Nanostructures and Their Hybrids for Advanced Energy and Environmental Applications: A Review. Journal of Nanoscience and Nanotechnology, 2019, 19, 307-331.	0.9	21
85	Temperature-dependent Raman studies and thermal conductivity of direct CVD grown non-van der Waals layered Bi2O2Se. Journal of Applied Physics, 2021, 129, .	1.1	21
86	Strain Anisotropy in Freestanding Germanium Nanoparticles Synthesized by Ball Milling. Journal of Nanoscience and Nanotechnology, 2009, 9, 5231-5236.	0.9	20
87	Size Dependent Anisotropic Strain and Optical Properties of Strained Si Nanocrystals. Journal of Nanoscience and Nanotechnology, 2011, 11, 9215-9221.	0.9	20
88	Plasmonic Metal and Semiconductor Nanoparticle Decorated TiO2-Based Photocatalysts for Solar Light Driven Photocatalysis. , 2018, , 786-794.		20
89	Strain analysis on freestanding germanium nanocrystals. Journal Physics D: Applied Physics, 2009, 42, 245402.	1.3	18
90	Density functional theory investigation of negative differential resistance and efficient spin filtering in niobium-doped armchair graphene nanoribbons. Physical Chemistry Chemical Physics, 2017, 19, 29685-29692.	1.3	18

#	Article	IF	CITATIONS
91	Compensating defect in deep buried layers produced by MeV heavy ions in n-silicon. Applied Physics Letters, 1997, 71, 1682-1684.	1.5	17
92	Tunable and High Photoluminescence Quantum Yield from Selfâ€Decorated TiO ₂ Quantum Dots on Fluorine Doped Mesoporous TiO ₂ Flowers by Rapid Thermal Annealing. Particle and Particle Systems Characterization, 2018, 35, 1800198.	1.2	17
93	Thermal stability of defect complexes due to high dose MeV implantation in silicon. Materials Science and Engineering B: Solid-State Materials for Advanced Technology, 2000, 71, 327-332.	1.7	16
94	Optical Signature of Structural Defects in Single Walled and Multiwalled Carbon Nanotubes. Journal of Nanoscience and Nanotechnology, 2009, 9, 5396-5401.	0.9	16
95	IMPROVED CHEMICAL SYNTHESIS OF GRAPHENE USING A SAFER SOLVOTHERMAL ROUTE. International Journal of Nanoscience, 2011, 10, 39-42.	0.4	16
96	Vacuum deposited PbI2 film grown at elevated temperatures for improved efficiency of CH3NH3PbI3 based planar perovskite solar cells. Materials Research Bulletin, 2021, 139, 111255.	2.7	16
97	High-Yield Chemical Synthesis of Hexagonal ZnO Nanoparticles and Nanorods with Excellent Optical Properties. Journal of Nanoscience and Nanotechnology, 2012, 12, 201-206.	0.9	15
98	Ti nanoparticles decorated ZnO nanowires heterostructure: photocurrent and photoluminescence properties. Journal of Experimental Nanoscience, 2013, 8, 332-340.	1.3	15
99	Early stages of growth of Si nanowires by metal assisted chemical etching: A scaling study. Applied Physics Letters, 2015, 107, .	1.5	15
100	Stable deep blue emission with unity quantum yield in organic–inorganic halide perovskite 2D nanosheets doped with cerium and terbium at high concentrations. Journal of Materials Chemistry C, 2021, 9, 2437-2454.	2.7	15
101	Low bias stress and reduced operating voltage in SnCl2Pc based n-type organic field-effect transistors. Applied Physics Letters, 2014, 104, .	1.5	14
102	Temperature-dependent Raman study and determination of anisotropy ratio and in-plane thermal conductivity of low-temperature CVD-grown PdSe ₂ using unpolarized laser excitation. Journal of Materials Chemistry C, 2021, 9, 16693-16708.	2.7	14
103	Emerging doping strategies in two-dimensional hybrid perovskite semiconductors for cutting edge optoelectronics applications. Nanoscale Advances, 2022, 4, 995-1025.	2.2	14
104	Formation and annealing of defects during high-temperature processing of ion-implanted epitaxial silicon: the role of dopant implants. Materials Science and Engineering B: Solid-State Materials for Advanced Technology, 2000, 71, 186-191.	1.7	13
105	EFFECT OF RAPID THERMAL ANNEALING ON MICROSTRUCTURE AND OPTICAL PROPERTIES OF ZnO NANORODS. International Journal of Nanoscience, 2011, 10, 65-68.	0.4	13
106	Study of the Suitability of Selected Extractants for Determination of Plant-Available Arsenic in Some Inceptisols of West Bengal, India. Communications in Soil Science and Plant Analysis, 2012, 43, 2449-2466.	0.6	13
107	Efficient visible light photocatalysis and tunable photoluminescence from orientation controlled mesoporous Si nanowires. RSC Advances, 2016, 6, 35365-35377.	1.7	13
108	Growth kinetics of hybrid perovskite thin films on different substrates at elevated temperature and its direct correlation with the microstructure and optical properties. Applied Surface Science, 2020, 530, 147224.	3.1	13

#	Article	IF	CITATIONS
109	Nonexponentiality in photoinduced current transients in undoped semiâ€insulating gallium arsenide. Journal of Applied Physics, 1995, 78, 262-268.	1.1	11
110	Studies on the surface swelling of ion-irradiated silicon: Role of defects. Materials Science and Engineering B: Solid-State Materials for Advanced Technology, 2005, 121, 238-243.	1.7	11
111	Intense Ultraviolet-Blue Photoluminescence from SiO ₂ Embedded Ge Nanocrystals Prepared by Different Techniques. Journal of Nanoscience and Nanotechnology, 2009, 9, 5389-5395.	0.9	11
112	Distinguishing defect induced intermediate frequency modes from combination modes in the Raman spectrum of single walled carbon nanotubes. Journal of Applied Physics, 2012, 111, .	1.1	11
113	Facile synthetic route to exfoliate high quality and super-large lateral size graphene-based sheets and their applications in SERS and CO2 gas sensing. RSC Advances, 2021, 11, 9488-9504.	1.7	11
114	Simultaneous formation of Si and Ge nanocrystals in SiO2 by one step ion implantation. Materials Science and Engineering B: Solid-State Materials for Advanced Technology, 2006, 128, 201-204.	1.7	10
115	Quantitative understanding of the ultra-sensitive and selective detection of dopamine using a graphene oxide/WS ₂ quantum dot hybrid. Journal of Materials Chemistry C, 2020, 8, 7935-7946.	2.7	10
116	Electrically active defects in as-implanted, deep buried layers inp-type silicon. Journal of Applied Physics, 1997, 81, 260-263.	1.1	9
117	Photoluminescence and structural studies on extended defect evolution during high-temperature processing of ion-implanted epitaxial silicon. Journal of Applied Physics, 2001, 89, 4310-4317.	1.1	9
118	Surface acoustic phonon modes of Ge nanocrystals embedded in SiO2. Solid State Communications, 2005, 136, 36-40.	0.9	9
119	Studies on Zinc Oxide Nanorods Grown by Electron Beam Evaporation Technique. Synthesis and Reactivity in Inorganic, Metal Organic, and Nano Metal Chemistry, 2007, 37, 437-441.	0.6	9
120	Strain dependence of the nonlinear optical properties of strained Si nanoparticles. Optics Letters, 2014, 39, 3833.	1.7	9
121	Low operating voltage and low bias stress in top-contact SnCl ₂ Pc/CuPc heterostructure-based bilayer ambipolar organic field-effect transistors. Journal of Materials Chemistry C, 2015, 3, 7118-7127.	2.7	9
122	Unusual features in trap emission characteristics of heavily damaged silicon induced by MeV ion implantation. Semiconductor Science and Technology, 2000, 15, 985-991.	1.0	8
123	Capacitance transient spectroscopy models of coupled trapping kinetics among multiple defect states: Application to the study of trapping kinetics of defects in heavy-ion-damaged silicon. Physical Review B, 2000, 62, 2496-2504.	1.1	8
124	Low energy oxygen implantation induced improved crystallinity and optical properties of surface modified ZnO single crystals. Applied Surface Science, 2009, 256, 384-388.	3.1	8
125	Effect of plasmonic metal nanoparticles on the performance of air processed inverted perovskite solar cells. AIP Conference Proceedings, 2019, , .	0.3	8
126	Exciton-plasmon coupling and giant photoluminescence enhancement in monolayer MoS ₂ through hierarchically designed TiO ₂ /Au/MoS ₂ ternary coreâ~'shell heterostructure. Nanotechnology, 2021, 32, 215201.	1.3	8

#	Article	IF	CITATIONS
127	Experimental and theoretical study of europium-doped organometal halide perovskite nanoplatelets for UV photodetection with high responsivity and fast response. Nanoscale, 2022, 14, 6402-6416.	2.8	8
128	Photoluminescence study of self-interstitial clusters and extended defects in ion-implanted silicon. Physica B: Condensed Matter, 2003, 340-342, 734-737.	1.3	7
129	EFFECT OF GROWTH TEMPERATURE ON THE CATALYST-FREE GROWTH OF LONG SILICON NANOWIRES USING RADIO FREQUENCY MAGNETRON SPUTTERING. International Journal of Nanoscience, 2011, 10, 13-17.	0.4	7
130	Co -DOPED ZnO NANOWIRES GROWN BY VAPOR–LIQUID–SOLID METHOD: STRUCTURAL, OPTICAL AND MAGNETIC STUDIES. Nano, 2012, 07, 1250028.	0.5	7
131	Label-free glucose detection over a wide dynamic range by mesoporous Si nanowires based on anomalous photoluminescence enhancement. Sensors and Actuators B: Chemical, 2018, 260, 693-704.	4.0	7
132	3D/2D Bi ₂ S ₃ /SnS ₂ heterostructures: superior charge separation and enhanced solar light-driven photocatalytic performance. CrystEngComm, 2021, 23, 2276-2288.	1.3	7
133	Self-catalytic growth of horizontal and straight Si nanowires on Si substrates using a sputter deposition technique. Solid State Communications, 2010, 150, 1923-1927.	0.9	6
134	Highly Suppressed Dark Current and Fast Photoresponse from Au Nanoparticle-Embedded, Si/Au/WS ₂ Quantum-Dot-Based, Self-Biased Schottky Photodetectors. ACS Applied Electronic Materials, 2021, 3, 4891-4904.	2.0	6
135	Ultrabroadband Absorption and High-Performance Photodetection in Europium-Doped 2D Topological Insulator Bi ₂ Se ₃ Nanosheets. ACS Applied Nano Materials, 2021, 4, 12527-12540.	2.4	6
136	Electrically active defects due to end-of-ion-range damage in silicon irradiated with MeV Ar+ ions. Nuclear Instruments & Methods in Physics Research B, 1996, 111, 285-289.	0.6	5
137	Studies on the formation of Si nanocrystals in SiO2 by Ge ion implantation. Nuclear Instruments & Methods in Physics Research B, 2006, 244, 56-59.	0.6	5
138	Ambient condition bias stress stability of vanadium (IV) oxide phthalocyanine based p-channel organic field-effect transistors. Journal Physics D: Applied Physics, 2018, 51, 015110.	1.3	5
139	Plasma-Treated Graphene Surfaces for Trace Dye Detection Using Surface-Enhanced Raman Spectroscopy. ACS Applied Nano Materials, 2022, 5, 6352-6364.	2.4	5
140	Evidence of metastability with athermal ionization from defect clusters in ion-damaged silicon. Physical Review B, 2000, 62, 16561-16565.	1.1	4
141	A comparative study of the vibrational and luminescence properties of embedded Ge nanocrystals prepared by ion implantation and sputter deposition methods: role of strain and defects. Semiconductor Science and Technology, 2007, 22, 1332-1338.	1.0	4
142	ROOM TEMPERATURE FERROMAGNETISM IN Co-DOPED ZnO NANOPARTICLES: MILLING TIME DEPENDENCE AND ANNEALING EFFECT. International Journal of Nanoscience, 2011, 10, 307-311.	0.4	4
143	Charge redistribution among defects in heavily damaged silicon. Physical Review B, 1998, 57, 14603-14606.	1.1	3
144	Metastablility of Interstitial Clusters in Ion-Damaged Silicon Studied by Isothermal Capacitance Transient Spectroscopy. Defect and Diffusion Forum, 2002, 210-212, 1-14.	0.4	3

#	Article	IF	CITATIONS
145	Electrical signature for configurational bistability of self-interstitial clusters in ion-damaged silicon. Physica B: Condensed Matter, 2003, 340-342, 729-733.	1.3	3
146	Correlating the microstructural and photoluminescence properties of ZnO nanoparticles prepared by ball milling. , 2007, , .		3
147	SHAPE EVOLUTION IN ONE-DIMENSIONAL ZnO NANOSTRUCTURES GROWN FROM ZnO NANOPOWDER SOURCE: VAPOR–LIQUID–SOLID VERSUS VAPOR–SOLID GROWTH MECHANISMS. International Journal of Nanoscience, 2011, 10, 75-79.	0.4	3
148	ORGANIC CuPc COATING INDUCED IMPROVED PHOTOLUMINESCENCE AND PHOTOCONDUCTIVITY OF ZnO NANOWIRES ARRAY. Functional Materials Letters, 2012, 05, 1250021.	0.7	3
149	Enhanced visible light photocatalysis by fluorine doped faceted TiO2 nanoflowers hierarchically designed with vacancy-rich TiO2 nanocrystals grown by vacuum annealing. AIP Conference Proceedings, 2019, , .	0.3	3
150	UV Photodetector Based on Graphene-ZnO Nanowire Hybrid: Fabrication, Photoresponse and Photoluminescence Studies. Advanced Science Letters, 2016, 22, 99-104.	0.2	3
151	Low-Temperature Chemical Vapor Deposition Growth of MoS2 Nanodots and Their Raman and Photoluminescence Profiles. Frontiers in Nanotechnology, 2021, 3, .	2.4	3
152	Defect Contribution to the Photoluminescence from Embedded Germanium Nanocrystals Prepared by Ion Implantation and Sputter Deposition Methods. Materials Research Society Symposia Proceedings, 2007, 994, 1.	0.1	2
153	Simultaneous photoluminescence enhancement in CVD grown single layer MoS2 and TiO2 NRs in the MoS2@TiO2 heterojunction. AIP Conference Proceedings, 2019, , .	0.3	2
154	Sensitivity of Electrically Active Defect Spectra to Processing Conditions in Mev Heavy Ion Implanted Silicon. Materials Research Society Symposia Proceedings, 1999, 568, 115.	0.1	1
155	Oxidation induced precipitation in Al implanted epitaxial silicon. Journal of Applied Physics, 2000, 88, 3988.	1.1	1
156	Quantitative Analysis of Diameter Dependent Properties of Multi-walled Carbon Nanotubes. , 2009, , .		1
157	EFFECT OF ZnO NANOPOWDER SOURCE AND GROWTH TEMPERATURE ON SHAPE EVOLUTION OF ZnO NANOSTRUCTURES. International Journal of Nanoscience, 2011, 10, 833-837.	0.4	1
158	DEFECT EVOLUTION AND STRUCTURAL IMPROVEMENT IN LOW ENERGY ION IRRADIATED CARBON NANOTUBES: MICROSCOPIC AND SPECTROSCOPIC STUDIES. International Journal of Nanoscience, 2011, 10, 49-53.	0.4	1
159	Fluorescence based comparative study of interaction of perylene with nitrogen doped graphene quantum dots and graphene oxide sheets. AIP Conference Proceedings, 2019, , .	0.3	1
160	Characterization of deep level defects in Si irradiated with MeV Ar+ ions using constant capacitance time analyzed transient spectroscopy. Bulletin of Materials Science, 1997, 20, 417-421.	0.8	0
161	Charge Redistribution and Defect Relaxation in Heavily Damaged Silicon Studied Using Time Analyzed Transient Spectroscopy. Materials Research Society Symposia Proceedings, 1998, 510, 349.	0.1	0
162	Radiative Versus Nonradiative Decay Processes in Germanium Nanocrystals Probed by Time-resolved Photoluminescence Spectroscopy. Materials Research Society Symposia Proceedings, 2005, 864, 4361.	0.1	0

#	Article	IF	CITATIONS
163	Novel Low Temperature Chemical Synthesis and Characterization of Zinc Oxide Nanostructures. Journal of Nanoscience and Nanotechnology, 2008, 8, 4290-4294.	0.9	Ο
164	High temperature ferromagnetism in Ni doped ZnO nanoparticles: Milling time dependence. , 2014, , .		0
165	High photoluminescence yield from organometal halide perovskite quantum dots confined in a mesoporous TiO2 template grown by rapid thermal annealing. AIP Conference Proceedings, 2019, , .	0.3	Ο
166	Effect of Rapid Thermal Annealing on the Photoluminescence from Si Nanocrystal Decorated Si Nanowires Array Grown by a Metal Assisted Chemical Etching Method. Advanced Science Letters, 2016, 22, 71-76.	0.2	0